15th Canadian Masonry Symposium
Ottawa, Canada
June 2-5, 2025

Seismic Performance Assessment and Fragility Analysis of Masonry Infilled RC Frames Using a New Macro Model

Nima Maymandi[i] and Yi Liu[ii]

ABSTRACT

This paper presents the results of seismic performance assessment of masonry infilled reinforced concrete frame systems. A macro model featuring bi-strut and a shear spring was implemented in OpenSees to simulate the seismic response of representative infilled system archetypes, each characterized by distinct design parameters. The analysis involved conducting incremental dynamic analysis utilizing a set of 30 pairs of strong ground motion records to obtain fragility curves of these archetypes. The performance of archetypes as indicated by fragility curves for Immediate Occupancy (IO), Life Safety (LS), and Collapse Prevention (CP) performance limit states was presented and discussed in this paper. The results augmented the database of numerical studies on seismic behaviour of masonry infilled frames. The impact of adding an infill on the seismic performance of the frame structure was shown. The seismic performance evaluated in this paper focuses on the strength of the frame structure. This study also shows the effect of several parameters such as location of soft storey on the seismic performance of infilled frames. The results also reveal that the infill design provisions in the current Canadian masonry design standard will lead to overestimate of infill strength in the context of seismic design.

KEYWORDS

Seismic Performance Assessment, masonry infilled frames, reinforced concrete frame, fragility curves, incremental dynamic analysis.

[i] Department of Civil and Resource Engineering, Dalhousie University, Halifax, NS, Canada, Maymandi@dal.ca
[ii] Department of Civil and Resource Engineering, Dalhousie University, Halifax, NS, Canada, Yi.liu@dal.ca

INTRODUCTION

Masonry infilled frame construction in North America commonly employs a steel or reinforced concrete (RC) structure with a masonry wall panel filled within. Masonry products, clay bricks or concrete masonry blocks, are popular choices of infill material due to their ready availability. When the masonry infill is designed to participate in the load sharing with its bounding frame, the resulting masonry infilled frame is intended to combine the flexural resistance of the frame and the shear resistance of the infill to achieve the system strength under lateral loading. The existing literature has demonstrated that masonry infills can significantly enhance structural strength, ductility, and energy dissipation of the frame system under static or quasi-static loading [1],[2]. However, if not designed and detailed properly, the negative effect of masonry infills was also significant. The infill wall was shown to lead to premature and brittle failure of RC columns, consequently diminishing the overall building's performance. In several recent earthquakes, masonry infills were shown to have suffered significant damage and also caused damage to surrounding frames [3]. To provide an accurate assessment of the infill-frame interaction and the impact of infills on the frame, a comprehensive seismic performance analysis of the masonry infilled frames is needed. The seismic performance assessment of infilled frame structures has received considerable attention in recent studies [4], [5], [6], [7], [8]. These seismic analyses were conducted by employing either a pushover or incremental dynamic analysis (IDA) technique through a computerized finite element model of the infilled frame structure. These studies showed that overall, the masonry infills, when distributed uniformly through the structure, mitigates the seismic fragility of the surrounding frame and enhance the specific performance of the frame structure. These studies also identified unique characteristics of seismic performance of masonry infilled frames with different design parameters. Del Gaudio et al. [5] showed that concrete block infills had higher median drift capacity than clay brick infills. Decanini [7] demonstrated, through a nonlinear dynamic analyses of infilled RC frame models, the vulnerability of soft storey frames in seismic performance of an infilled frame. Burton and Deierlein [8] underscored the critical role of strong infills played in shear failure of frame columns which in turn resulted in structure collapse. Mohammadi et al. [9] showed that, at lower performance levels, the masonry infill provided some beneficial effects, but at severe levels, these benefits diminished, and in the Collapse Prevention state, infills weakened the seismic performance of the steel frame. Since most of these existing studies conducted the seismic analysis through a finite element model, the accuracy of the results is largely dependent on the accurate representation of the model of the behaviour of the infilled frame. One limitation observed in these studies is that none of the employed numerical models predict the shear failure in the masonry infills. Maymandi [10] developed a macro-model to aid the lateral behaviour analysis of all-masonry infilled frames. The model was shown to be capable of accurately simulating the behaviour and capacity of masonry infilled RC frames under both static and cyclic loading. This paper focuses on the seismic performance assessment of masonry infilled RC frames using the developed numerical model. In this paper, seven archetypes, including three two-storey frames and four five-storey frames, were considered through an extensive series of Incremental Dynamic Analyses (IDAs). Additionally, this study introduced a logical approach for obtaining IDA curves for models with soft first stories by utilizing appropriate drift values. The resulting fragility curves for three distinct performance limit states: Immediate Occupancy (IO), Life Safety (LS), and Collapse Prevention (CP), were presented and discussed for the archetypes.

SUMMARY OF PROPOSED MODEL

A finite element model was developed to perform this seismic analysis [10]. The proposed model consists of four diagonal struts connected in the middle of the infill wall panel with a shear spring (Figure 1). The diagonal struts are compression-only trussed elements and intended to represent the compressive behaviour of the infill. The shear spring is a zero-length member and is intended to capture the shear sliding failure of the infill. The four more struts in dotted lines indicate the struts to account for the reverse loading. The total width of the two diagonal struts in either the upper or lower infill panel was determined based on the infill design provisions specified in the Canadian masonry design standard CSA S304-24 [11]. This width was then equally divided between the two struts. The contact point between the struts and columns was assumed as a fraction of the contact length as specified in CSA S304-24. The compressive struts and shear spring were arranged in a serial manner and the failure of either component led to the failure of the entire infill panel.

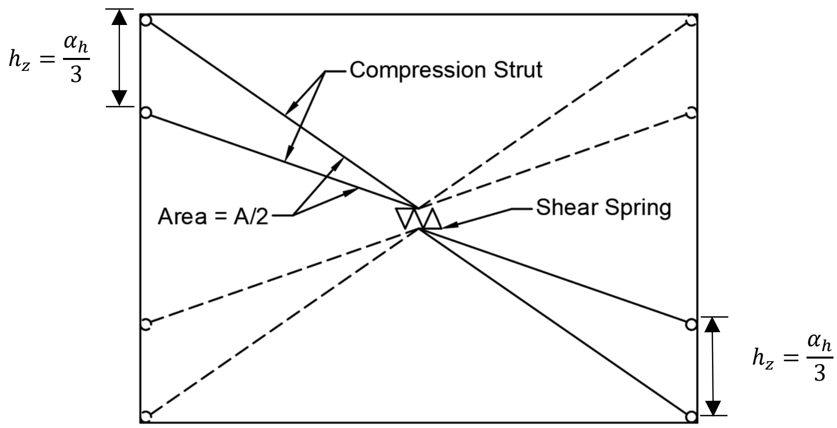

Figure 1: Proposed Bi-strut Spring Model

The proposed model was verified against experimental pushover and cyclic tests of masonry infilled RC frames, with and without openings. The results showed the model's effectiveness in capturing the failure modes in infilled frames including compression and sliding shear failure of the infill, as well as frame failure. One example verification is reproduced in Figure 2 where the numerical model results are compared with experimental results obtained by Kakaletsis and Karayannis on an infill wall with a central window opening subjected to cyclic lateral loading [12].

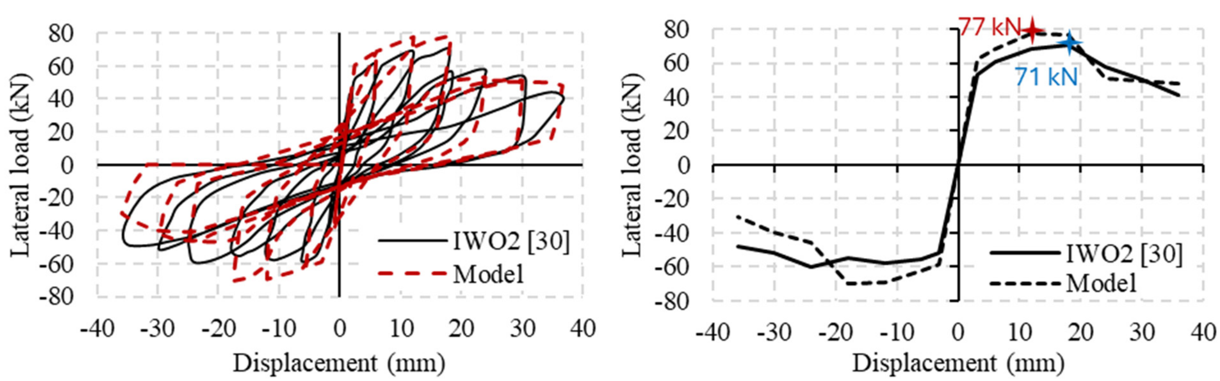

Figure 2: Comparison of Hysteretic Response and Backbone Curve of the Proposed Numerical Model and Specimens IWO2 Tested by Kakaletsis and Karayannis (2008)

SEISMIC STUDY ARCHETYPES

Seven frame structure archetypes were developed and used in the seismic analysis. The analysis was conducted in two distinctive studies. In Study I, three two-storey archetypes were analyzed where: one having no infills (bare frame), one with the infills modelled using the CSA S304 single-strut method, and one with the infills modelled using the proposed model, as shown Figure 3. In Study II, two two-bay, five-storey archetypes were analyzed where one group was used to investigate the effect of soft storey at different locations of the structure, as shown in Figure 4. These models were originally designed to meet the structural requirements of the city of Vancouver, considering a soil classification of Type C.

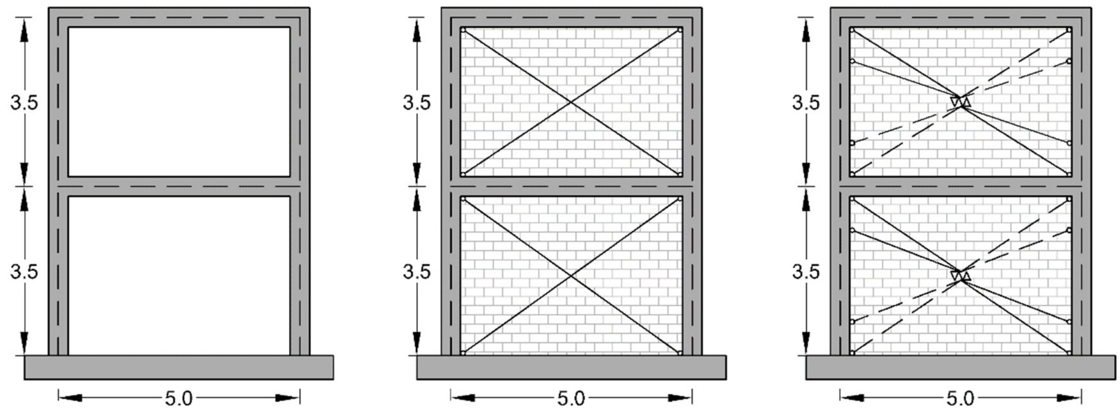

a) 2-BF　　b) 2-CSA　　c) 2-Proposed

Figure 3: Study I Models (Dimension Unit: M): a) 2-Storey Bare Frame (2-BF), b) 2-Storey Modeled Using CSA (2-CSA), c) 2-Storey Modeled Using Proposed Model (2-Proposed)

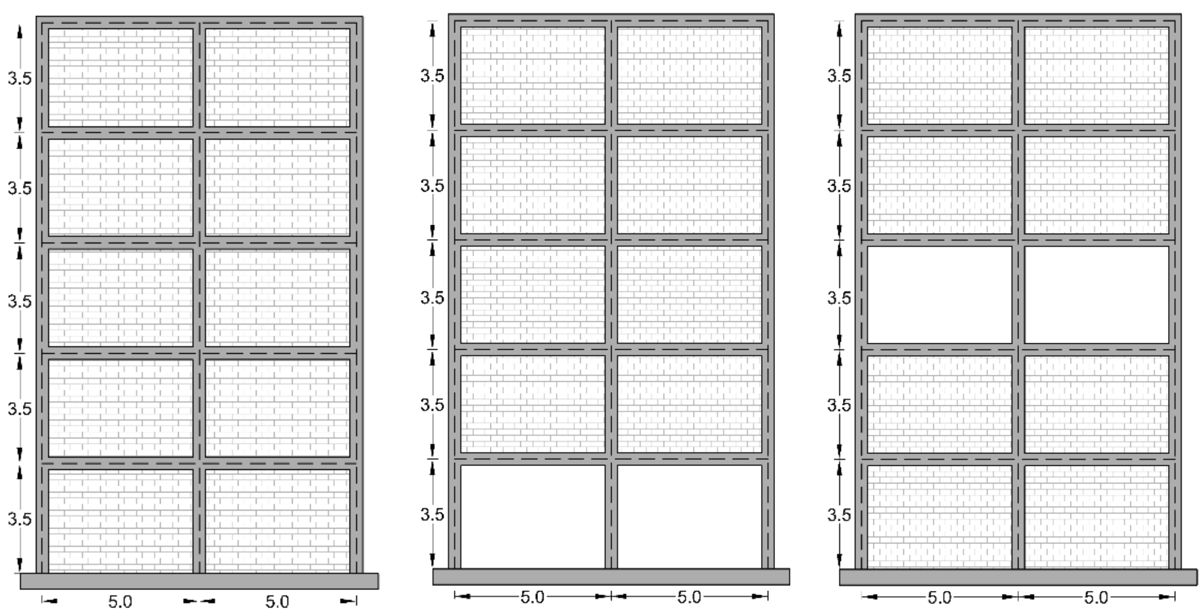

a) 5-IW-0.7　　b) 5-SS1　　c) 5-SS3

Figure 4: Study II Models (Dimension Unit: M): a) 5-Storey with Aspect Ratio 0.7 (5-IW-0.7), b) 5-Storey with Soft Storey at First Floor(5-SS1), c) 5-Storey with Soft Storey at Third Floor (5-SS3)

For all archetypes, the infill was assumed to be constructed with 200 mm standard concrete masonry units, ungrouted. The masonry properties for infills and concrete properties for bounding frames were kept the same for all models, with details summarized in Table 1. The bounding frame dimensions and reinforcement situations are shown in Table 2.

Table 1: Summary of Material Properties of Archetypes

	Material properties	
Masonry infill	Compressive strength (f'_m)	13 MPa
	Elastic modulus (E_m)	11050 MPa
RC bounding frame	Compressive strength (f'_c)	30 MPa
	Elastic modulus (E_c)	25750 MPa
	Yield strength of steel (f_y)	425 MPa
	Ultimate strength of steel (f_u)	650 MPa

Table 2: Cross-section of Frames for Each Study

<table>
<tr><th colspan="2"></th><th>Column (mm)</th><th>Beam (mm)</th></tr>
<tr><td colspan="2">Study I frame</td><td>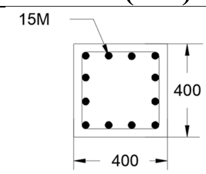
</td><td>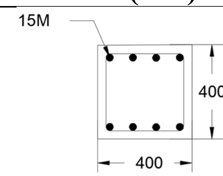
</td></tr>
<tr><td rowspan="2">Study II frame</td><td>Storey 4 & 5</td><td>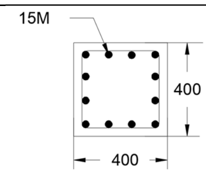
</td><td>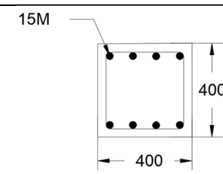
</td></tr>
<tr><td>Storey 1, 2 & 3</td><td>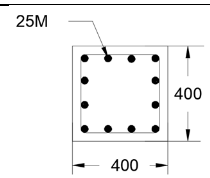
</td><td>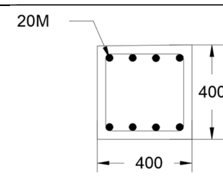
</td></tr>
</table>

INCREMENTAL DYNAMIC ANALYSIS (IDA)

The study utilized Incremental Dynamic Analysis (IDA), a technique originally proposed by Bertero, to assess structural responses under seismic loads. IDA involves conducting multiple nonlinear dynamic analyses on structural models using real ground motion data. These analyses incrementally increase the intensity of ground motions to observe structural responses ranging from elastic behavior to potential collapse. The resulting data is used to evaluate seismic performance probabilistically. Key components of the IDA methodology, as defined by Vamvatsikos and Cornell [13], include terms like scale factors (SF), Intensity Measures (IM), Damage Measures (DM), IDA curves, Single-Record IDA curves, and Multi-Record IDA curves. Single-Record IDA curves (Dynamic Pushover curves) represent the relationship between DM (e.g., maximum inter-storey drift) and IM (e.g., spectral acceleration) for a single ground motion, incrementally increasing in intensity. Multi-Record IDA curves aggregate data from multiple ground motions to capture a broader range of structural responses. The slope of an IDA curve is an indicator of structural behavior. A linear slope indicates an elastic response, where DM and IM are proportional. Nonlinear slopes reflect damage and yielding, while flat slopes indicate structural collapse due to analysis convergence failure. Proper ground motion selection is critical for generating comprehensive Multi-Record IDA curves, requiring sufficient records to represent the full spectrum of structural behaviors.

Selection of Ground Motion Records

The seismic study of this paper was assumed to be carried out in the province of British Columbia. British Columbia (BC) is in a seismic region characterized by moderate to high seismic activity. A set of 30 earthquakes with moment magnitudes between 6.8 and 8.1 used in the study by Taylor et al. [14], was also adopted in this investigation. They selected these ground motions for the cities of Vancouver and Victoria on soil corresponding to a C class. According to ASCE 7 [15], the average spectral acceleration of the 60 motions must exceed the design spectrum acceleration for the location within the range of 0.2 to 1.5 times the building's fundamental period (T_1). Table 4 summarizes T_1, 0.2 T_1, 1.5T_1, and the design spectral acceleration for each archetype. The ground motions were scaled to meet ASCE 7 requirements, minimizing disparities between the design response spectrum and the generated spectrum. Adjustments were made using Hancock et al. [16] and Al Atik and Abrahamson [17] algorithms via SeismoMatch software. Fig. 5(a) shows the response spectral acceleration of the original 60 ground motions, with the red line representing Vancouver's design spectrum. Ground motions were scaled to align with the design spectrum based on each archetype's T_1. For example, Fig. 5(b) illustrates the design spectrum for archetype 5-IW-0.7, matched to ground motions at T_1=0.65s.

Table 3: First Mode Period and Matching Intervals for All Archetype Models

Archetype	Fundamental period (T_1)	$0.2T_1$ (Sec)	$1.5T_1$ (Sec)	Design spectral acceleration (g)
2-BF	0.48	0.096	0.72	0.75
2-CSA	0.31	0.062	0.465	0.81
2-Proposed	0.38	0.076	0.57	0.79
5-IW-0.7	0.65	0.13	0.975	0.65
5-IW-0.5	0.61	0.122	0.915	0.68
5-SS1	0.73	0.146	1.095	0.60
5-SS3	0.70	0.14	1.05	0.62

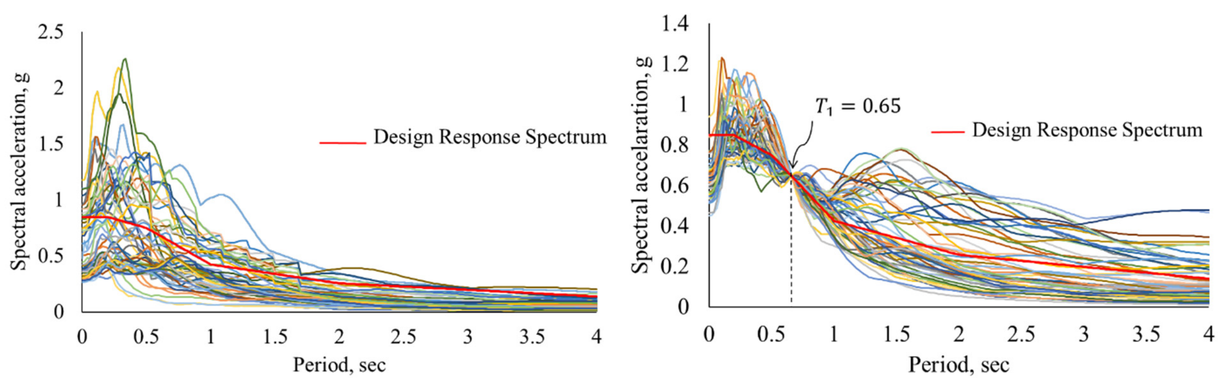

Figure 5: Response Spectrum for: a) The Original Selected Ground Motions and b) 5-IW-0.7 after Adjustment to the Ground Motion Records

Results of IDA

To develop IDA curves, a Damage Measure (DM) for the structure and an Intensity Measure (IM) for the ground motion are required. Here, $S_a(T_1, 5\%)$, the first mode spectral acceleration, was the IM, and the maximum inter-storey drift ratio, θ_{max}, the DM. Each ground motion was scaled into 20 incremental recordings from 0 to 4g. Figure 6(a) shows all IDA curves of archetype 5-IW-0.7 under 60 ground motions. Figure 6(b) plots the 16%, 50%, and 84% fractiles of DM for each IM value. At $S_a(T_1, 5\%)$ = 1g, 16% of records result in θ_{max}≤0.68, 50% in θ_{max}≤1.45 and 84% in θ_{max}≤1.96%. Figure 6(c) compares median curves of Study I (2-storey) models. Infill walls doubled the initial stiffness of the bare frame, reducing inter-storey drift for a given IM. Both proposed and CSA S304 models followed similar DM-IM trends, but the CSA S304 model overestimated stiffness and strength, predicting 3.4 times higher stiffness versus 1.6 times for the proposed model. The discrepancy arises because in the CSA S304 provision, the stiffness was only modelled from the infill compression failure, while the proposed model also includes shear failure.

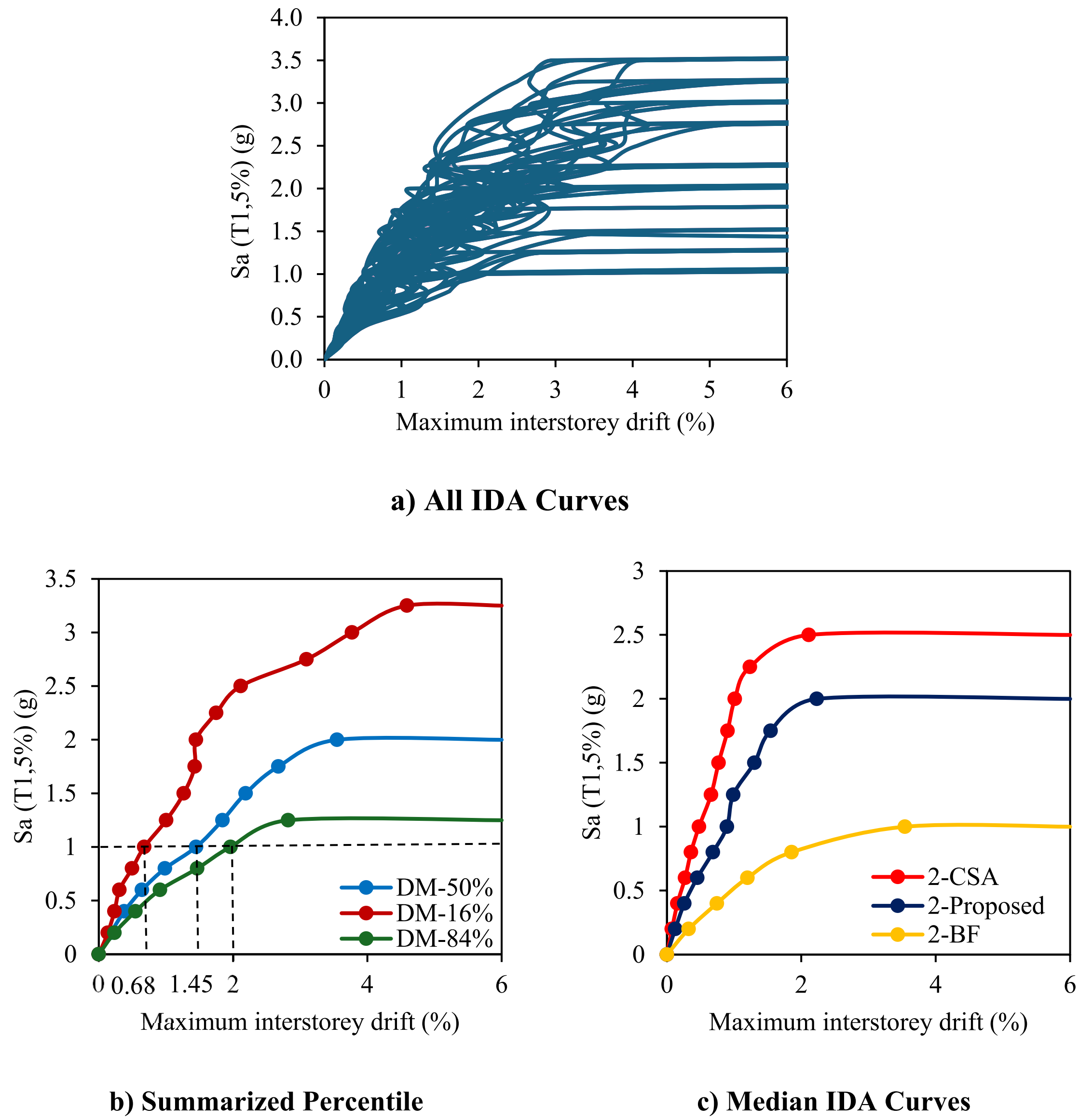

Figure 6: IDA Results

Figure 7 shows the effect of a soft storey in infilled frames. A soft storey reduces initial stiffness and increases inter-storey drift, with its location impacting severity. A soft storey on the first floor caused greater stiffness reduction and drift increase than one on the third floor. Model 5-SS1 (soft storey on the 1st floor) had a median collapse strength of $S_a(T_1, 5\%)$ =1.25g, compared to 2.0g for 5-IW-0.7 (no soft storey). For 5-SS3 (soft storey on the 3rd floor), the collapse strength was $S_a(T_1, 5\%)$ =1.5g, 20% higher than 5-SS1.

The greater impact of a first-floor soft storey stems from its critical role in resisting seismic loads, leading to larger displacements and earlier collapse.

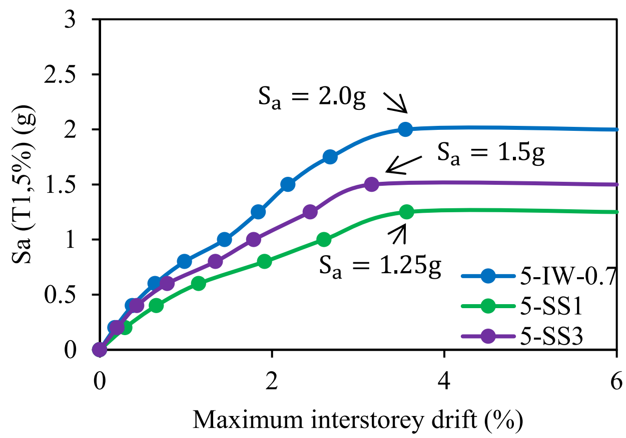

Figure 7: Median IDA Curves of Study II archetypes: Effect of Soft Storey

FRAGILITY ASSESSMENT

Fragility assessment uses fragility curves to estimate the probability of a structure exceeding specific performance levels under a given intensity measure (IM). This study developed curves for three performance limit states: Immediate Occupancy (IO), Life Safety (LS), and Collapse Prevention (CP). For CP, the study used FEMA's IM-based definition, marking collapse at the IDA curve's last point where the slope equals 20% of the elastic slope. This approach avoids ambiguities in DM-based definitions, which rely on predetermined DM values but may lead to overlapping IDA curve points. The IO and LS definitions for masonry-infilled frames were adopted from Jeon et al [18]. For IO, the yield point corresponds to a 0.16% drift, while LS corresponds to the maximum lateral force at a 0.49% drift. These values are based on analyses of 160 reinforced concrete frames with masonry infills. Based on the results of Incremental Dynamic Analysis (IDA) curves for the 60 ground motion records, the percentage of records exceeding a limit state as described above for a specific Intensity Measure (IM) level is presented as a fragility curve. Figure 8 illustrates the fragility curves of the 2-Proposed and 5-IW-0.7 archetypes in terms of the probability of exceedance versus $S_a(T_1, 5\%)$ for all three performance limit states. As anticipated, the probability of a frame reaching the Immediate Occupancy (IO) limit state is significantly higher than the probability of a frame reaching the Life Safety (LS) and Collapse Prevention (CP) states. The fact that LS and IO performance limit states are closely situated implies that these states occur within a narrow range of incremental Intensity Measures (IM). Most frames, after an increase in the load beyond the IO limit state, quickly reach the Life Safety limit state (LS). For instance, Figure 8(a) demonstrates that at $S_a(T_1, 5\%) = 1g$, the frame model 5-IW-0.7 has exceeded the IO state under all ground motion record and 81% of them have surpassed the LS limit state, and 11% have surpassed the CP state. The comparison of Figure 8(a) and (b) shows that the increase in the number of storeys does not significantly alter the probability of exceedance of a limit state.

Figure 9 compares the fragility curves for the Collapse Prevention (CP) limit state for Study I and II archetypes respectively. It can be seen that for most archetypes, the likelihood of surpassing the CP limit state under ground motions with an Intensity Measure (IM) up to 0.6g is nearly 0%. However, the likelihood of surpassing the CP limit state for 2-BF at $S_a(T_1, 5\%) = 0.6g$ is about 9% and for 5-SS1 is 4%. The fragility

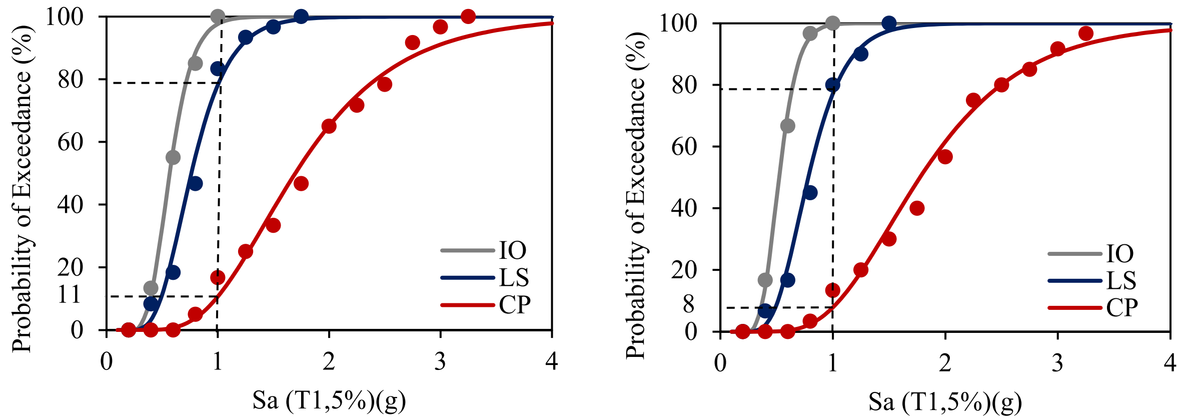

a) 5-IW-0.7 **b) 2-Proposed**

Figure 8: Comparison of Fragility Curves for 2-Proposed and 5-IW-0.7

curves for two-storey archetypes reflect the effects of different design approaches

Figure 9(a)). Notably, the CSA S304-24 approach resulted in a lower probability of exceeding the CP limit state. This is owning to the much stiffer system yielded by using the CSA S304-14 design method which in turn will require greater lateral forces to trigger performance limit states. This suggests that for low-rise structures, the CSA S304-24 design provisions may overestimate the contribution of infill walls under seismic loading, potentially leading to an unconservative assessment of the system's seismic behaviour.

Figure 9(b) illustrates that, compared to the soft first-story frame (model 5-SS1), the fully infilled frame exhibited better seismic performance across the entire IM range. For instance, the presence of a soft storey on the first floor at $S_a(T_1, 5\%) = 1g$ resulted in an increase in the probability of exceedance from 10% to 40%. In the case of having a soft storey on the third floor, the probability of exceedance was about 15%. The effect is less pronounced than having the soft storey on the first floor.

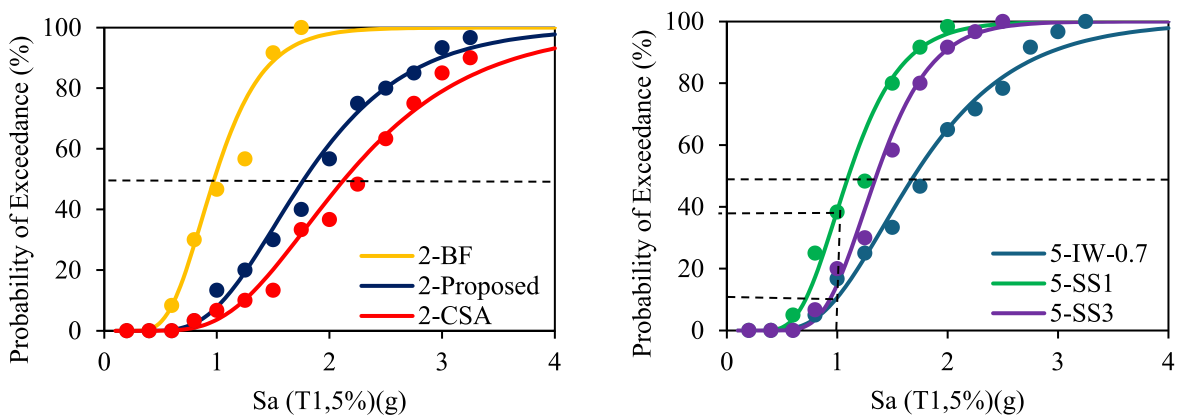

a) Study I: 2-storey structure **b) Study II: effect of soft storey**

Figure 9: Fragility Curves of All Models for CP Performance Limit States

Table 4 summarizes the median values of fragility curves for all frame models. These values were obtained using

Figure 9 as indicated by the dotted lines at 50% probability of exceedance level. To compare these models in different performance limit states, the relative change in median values of fragility curve were investigated. In the case of Study I, where 2-storey archetypes were compared to the bare frame model, it is observed that, for a more severe limit state, the infill has a lesser impact on the S_a associated with a 50% probability of exceeding the limit state, although it still significantly contributes to load sharing. All masonry-infilled frame models displayed higher median values across all three performance limit states when compared to the bare frame model. In Study II, the 5-storey archetypes were compared to the fully infilled frame model (5-IW-0.7). The table further reveals that having a soft storey had a lesser impact in the IO state and significantly altered the strength in the CP state and having a soft storey on the first floor had the lowest S_a for 50% probability of exceedance.

Table 4: Median (50%) Values of Fragility Curves for All Frame Models in Different Performance Limit States

	S_a			$S_{a,infill}/S_{a,2-BF}$		
Frame model	IO (g)	LS (g)	CP (g)	IO	LS	CP
2-BF	0.18	0.37	0.98	-	-	-
2-Proposed	0.52	0.78	1.78	2.89	2.11	1.82
2-CSA	0.68	0.99	2.13	3.78	2.68	2.17
				$S_a/S_{a,5-IW-0.7}$		
5-IW-0.7	0.55	0.76	1.69	-	-	-
5-SS1	0.48	0.61	1.11	0.87	0.80	0.66
5-SS3	0.52	0.66	1.36	0.95	0.87	0.8

CONCLUSION

This study presents results of seismic performance assessment of reinforced concrete (RC) frames with masonry infill walls. The seismic analysis was performed using a bi-strut-spring macro model developed by the authors through software OpenSees. Seven RC infilled frame archetypes were considered in this study including two-storey and five-storey configurations, designed to study the impact of different modeling approaches (CSA S304 or Proposed model), and the location of soft storeys in buildings. Through Incremental Dynamic Analysis (IDA), median IDA curves and fragility curves were obtained for different performance limit states—Immediate Occupancy (IO), Life Safety (LS), and Collapse Prevention (CP). It was found that for all infilled frame archetypes, the likelihood of exceeding the CP limit state under ground motions with intensity measures up to 0.6g is nearly 0%. The study suggests that the number of storeys in a building has a limited impact on seismic performance. The addition of infill walls to a bare frame was shown to significantly increase the seismic performance of the structure. However, the CSA S304-24 infill design approach tends to overestimate this benefit. A specific provision to address seismic design of masonry infills needs to be developed. The study also reveals that having a soft storey reduces seismic performance by almost half, with the soft storey's location being critical, especially when situated on the first floor. In summary, the paper underscores the gap in recognizing the impact of infill walls on RC frames, emphasizing the need to consider them as integral components for enhanced structural performance and resilience in seismic-prone regions. Further numerical analyses on RC infilled frames with varying material and geometric properties, alongside additional experimental tests under seismic loading conditions are recommended for future research.

ACKNOWLEDGEMENT

The authors wish to gratefully acknowledge the contribution of the financial assistance provided by the Natural Sciences and Engineering Research Council (NSERC) of Canada and the Canadian Concrete Masonry Producers Association for conducting this research.

REFERENCES

[1] Mehrabi, A.B., Benson Shing, P., Schuller, M.P., Noland, J.L., 1996. Experimental evaluation of masonry-infilled RC frames. Journal of Structural engineering 122, 228–237.
[2] Asteris, P.G., Chrysostomou, C.Z., Giannopoulos, I.P., Smyrou, E., 2011b. Masonry infilled reinforced concrete frames with openings. In: III ECCOMAS Thematic Conference on Computational Methods in Structural Dynamics and Earthquake Engineering. pp. 25–28.
[3] Ozkaynak, H., Yuksel, E., Yalcin, C., Dindar, A.A., Buyukozturk, O., 2014. Masonry infill walls in reinforced concrete frames as a source of structural damping. Earthq Eng Struct Dyn 43, 949–968.
[4] De Risi, M.T., Del Gaudio, C., Ricci, P., Verderame, G.M., 2018. In-plane behaviour and damage assessment of masonry infills with hollow clay bricks in RC frames. Eng Struct 168, 257–275.
[5] Del Gaudio, C., De Martino, G., Di Ludovico, M., Manfredi, G., Prota, A., Ricci, P., Verderame, G.M., 2019. Empirical fragility curves for masonry buildings after the 2009 L'Aquila, Italy, earthquake. Bulletin of earthquake engineering 17, 6301–6330.
[6] Gesualdi, G., Viggiani, L.R.S., Cardone, D., 2020. Seismic performance of RC frame buildings accounting for the out-of-plane behavior of masonry infills. Bulletin of Earthquake Engineering 18, 5343–5381.
[7] Decanini, L., Mollaioli, F., Mura, A., Saragoni, R., 2004. Seismic performance of masonry infilled R/C frames. In: 13th World Conference on Earthquake Engineering. Citeseer.
[8] Burton, H., Deierlein, G., 2014b. Simulation of Seismic Collapse in Nonductile Reinforced Concrete Frame Buildings with Masonry Infills. Journal of Structural Engineering 140.
[9] Mohammadi, M., Mirzaei, M., Pashaie, M.R., 2021. Seismic performance and fragility analysis of infilled steel frame structures using a new multi-strut model. In: Structures. Elsevier, pp. 1403–1415.
[10] Maymandi, N., 2024. Study of Seismic Behaviour of Masonry Infilled RC Frames, Dalhousie University.
[11] Canadian Standards Association (CSA), 2024. Design of masonry structures, CSA S304-24. ed. Mississauga, ON, Canada.
[12] Kakaletsis, D.J., Karayannis, C.G., 2008b. Influence of masonry strength and openings on infilled R/C frames under cycling loading. Journal of Earthquake Engineering 12, 197–221.
[13] Vamvatsikos, D., Cornell, C.A., 2002. Incremental dynamic analysis. Earthq Eng Struct Dyn 31, 491–514.
[14] Taylor, G., Ventura, C.E., Pina, F., Finn, W.D.L., 2010. Performance-based retrofit of school buildings in British Columbia, Canada. In: Improving the Seismic Performance of Existing Buildings and Other Structures. pp. 234–245.
[15] ASCE 7-22, 2022. Minimum design loads and associated criteria for buildings and other structures. American Society of Civil Engineers.
[16] Hancock, J., Watson-Lamprey, J., Abrahamson, N.A., Bommer, J.J., Markatis, A., McCoy, E., Mendis, R., 2006. An improved method of matching response spectra of recorded earthquake ground motion using wavelets. Journal of earthquake engineering 10, 67–89.
[17] Al Atik, L., Abrahamson, N., 2010. An improved method for nonstationary spectral matching. Earthquake spectra 26, 601–617.

[18] Jeon, J., Park, J., DesRoches, R., 2015. Seismic fragility of lightly reinforced concrete frames with masonry infills. Earthq Eng Struct Dyn 44, 1783–1803.